

Microwave Spectra and the Molecular Structure of Tetracarbonylethyleneiron

Brian J. Drouin and Stephen G. Kukolich*

Contribution from the Chemistry Department, University of Arizona, Tucson, Arizona 85721

Received November 12, 1998

Abstract: Microwave spectra of seven isotopomers of tetracarbonylethyleneiron were recorded using a Pulse-Beam Fourier Transform Microwave Spectrometer. Rotational transitions for a “c” dipole moment with $J' \leftarrow J$ from $2 \leftarrow 1$ to $6 \leftarrow 5$ were measured in the 4–12 GHz range. Rotational constants were determined by fitting the measured microwave spectra to a Watson “A” reduced Hamiltonian with centrifugal distortion parameters. The measured rotational constants of the main isotopomer are $A = 1031.1081(4)$ MHz, $B = 859.8055(4)$ MHz, and $C = 808.5675(3)$ MHz. Data were also obtained for three ^{13}C -substituted species and two ^{18}O -substituted species in natural abundance. Additional spectra were measured for an isotopically enriched sample of perdeuterated tetracarbonylethyleneiron. The moments of inertia of the seven isotopomers were used in a Kraitchman analysis and in two different least-squares fitting analyses to determine the molecular structure of the compound. The ethylene ligand exhibits significant structural changes upon complexation to iron, primarily an increase in C–C bond length with movement of the hydrogen atoms away from the metal center. The C–C and C–H bond lengths were found to be $r_o = 1.419(7)$ and $= 1.072(4)$ Å, respectively. The C–C–H angle and the Fe–C–C–H dihedral angle were found to be $\angle(\text{C–C–H})_o = 120.6(5)^\circ$ and $\angle(\text{Fe–C–C–H})_o = 103.6(9)^\circ$, respectively. The plane of the hydrogen atoms is displaced $0.217(2)$ Å above the ethylene carbon atoms, along the c axis. Extensive DFT calculations were carried out prior to the experimental research. The calculated structure proved extremely valuable in obtaining accurate predictions for the spectra, and provided structural parameters in excellent overall agreement with measured parameters.

Introduction

Olefin activation on metal catalysts is often used today in organic^{1–5} syntheses. The commonly accepted mechanisms⁶ for olefin isomerization involve metallocyclopropane intermediate complexes. These short-lived intermediates are quickly converted to either allylic or alkyl bound intermediates or released from the metal to give a free olefin. Experiments are often carried out on closely related model compounds since reaction intermediates are notoriously difficult to study. In many cases, the most closely related model compounds are still quite reactive. This is certainly the case for the present example, tetracarbonylethyleneiron.^{7,8} The ethylene ligand is very labile in this compound as indicated by rapid decomposition under light to form $\text{Fe}_3(\text{CO})_{12}$. This compound is an example of a simple metal bound olefin complex since it contains only one olefinic bond formed from π and π^* orbitals interacting with d orbitals on the metal center. The characteristics and reactivity of typical metal–olefin bonds^{9,10} are well represented in this

simple complex. An early electron diffraction study¹¹ (GED) verified the basic trigonal bipyramidal structure, and this was supported by the assignment of the vibrational spectrum.¹² The ethylene is bound on one of the equatorial sites of a near trigonal bipyramidal structure, the C–C bond lies in the equatorial plane, and the molecule has C_{2v} symmetry with the C_2 rotation axis bisecting the olefin bond. Unfortunately, the GED structure¹¹ does not provide hydrogen coordinates, and there were difficulties in locating hydrogen atoms for an X-ray study^{8,13} of a similar compound. This solid-state X-ray structure is for the closely related compound^{8,13} $\text{Fe}(\text{P}(\text{C}_6\text{H}_5)_3)(\text{CO})_3\text{C}_2\text{H}_4$. This X-ray structure includes a reasonable Fe–C–C–H dihedral angle but the C–H distances are not well determined, indicating that the direction of the bond was determined more accurately than the length. No X-ray study of the title compound was found in the literature, presumably because of the high sensitivity to light, heat, and air. Accurate hydrogen coordinates for this molecule are important because structural changes of the ethylene upon complexation help to indicate how much the metal center can activate the olefin. In a previous study, accurate coordinates for the hydrogen atoms provided evidence for a dramatic change in hybridization from sp^2 to near sp^3 for the terminal H atoms of butadiene, when complexed to iron.¹⁴ The X-ray structure of $\text{Fe}(\text{P}(\text{C}_6\text{H}_5)_3)(\text{CO})_3\text{C}_2\text{H}_4$ indicates that the C–H bonds are bent 8° out of the (former) ethylene plane. This suggests that a similar hybridization change occurs for the

- (1) Miller, M. E.; Grant, E. R. *J. Am. Chem. Soc.* **1985**, *107*, 3386.
- (2) Wu, Y.; Bensten, J. G.; Brinkley, C. G.; Wrighton, M. S. *Inorg. Chem.* **1987**, *26*, 530.
- (3) Kane, V. V.; Light, J. R.; Whiting, M. C. *Polyhedron* **1985**, *4*, 533.
- (4) Roberts, B. W.; Wong, J. *J. Chem. Soc., Chem. Commun.* **1977**, 20.
- (5) Baar, M. R.; Roberts, B. W. *J. Chem. Soc., Chem. Commun.* **1979**, 1129.
- (6) Crabtree, R. H. *The Organometallic Chemistry of the Transition Metals*; Wiley-Interscience Inc.: New York, 1994; Chapter 9.
- (7) Murdoch, H. D.; Weiss, E. *Helv. Chem. Acta* **1963**, *66*, 1588.
- (8) Lindner, E.; Schauss, E.; Hiller, W.; Fawzi, R. *Angew. Chem., Int. Ed. Engl.* **1984**, *23*, 711.
- (9) Barnhart, T. M.; Fenske, R. F.; McMahon, R. J. *Inorg. Chem.* **1992**, *31*, 2681.
- (10) Beach, D. B.; Jolly, W. L. *Inorg. Chem.* **1983**, *22*, 2137.

- (11) Davis, M. I.; Speed, S. *J. Organomet. Chem.* **1970**, *21*, 401.
- (12) Andrews, D. C.; Davidson, G. *J. Organomet. Chem.* **1972**, *35*, 161.
- (13) Lindner, E.; Schauss, E.; Hiller, W.; Fawzi, R. *Chem. Ber.* **1985**, *118*, 39 15.
- (14) Kukolich, S. G.; Roehrig, M. A.; Wallace, D. W.; Henderson, G. L. *J. Am. Chem. Soc.* **1993**, *115*, 2021.

ethylene ligand. Numerous theoretical studies^{15–17} have been performed to assess the degree to which the tetracarbonyl iron fragment can activate olefins. When detailed structural data are available, the accuracy of the theoretical analyses can be better evaluated. Further exploitation of the theory may help to elucidate the remarkable properties of this molecule, including a rich photochemistry,¹⁸ and catalytic activity in the isomerization of alkenes.²

The title compound is structurally similar to the series of dihydrides^{19–21} previously studied by this group, particularly $\text{H}_2\text{Fe}(\text{CO})_4$.²⁰ The ethylene replaces the two hydride ligands bound to the tetracarbonylferrate base. Both of these molecules are thermal, light, and air sensitive. Chemically, the molecule is much more similar to the η^4 - and η^5 -bound Fe systems also studied by microwave spectroscopy.^{14,22–25} The tricarbonylcyclobutadieneiron,^{11,21} tricarbonylbutadieneiron,^{11,14} and tricarbonylcyclooctatetraeneiron²³ species are all η^4 type “piano-stool” complexes with increasing stability in the order listed. The sandwich compounds chloro- and bromoferrocene^{24,25} are both very stable in comparison with the diene–iron–carbonyls, but are less stable than the parent compound, ferrocene. Complete gas-phase structures have been published for $\text{H}_2\text{Fe}(\text{CO})_4$ ¹⁹ and $\text{C}_4\text{H}_5\text{Fe}(\text{CO})_3$ ¹⁴ along with some structural data for $\text{C}_4\text{H}_4\text{Fe}(\text{CO})_3$ ²¹ and the haloferrocenes.^{24,25} Previous electron diffraction¹¹ work has shown that structural comparisons between these species provide valuable insight into the characteristics of the compounds and their reactivity. In the present work microwave spectra for a large number of isotopomers are given and a very detailed structure of the η^2 -bound ethylene complex is presented. The experimental results, along with the DFT calculations performed, provide a more complete view of structure and bonding for the olefin–iron systems.

Density functional calculations are becoming increasingly accurate and useful for describing structures of organometallic systems. Previously the BPW91²⁶ methods of Gaussian²⁷ were shown to reproduce the gas-phase structure of $\text{H}_2\text{Fe}(\text{CO})_4$ ¹⁹ with great accuracy. It is useful to test the accuracy of quantum chemical theories with relatively small systems to determine if their application to larger structures is valid. Many of the iron systems studied in this laboratory have been modeled using DFT

calculations in an effort to further test the application of DFT in predicting gas-phase structures of organometallic complexes.

Experimental Section

The sample was prepared using the method of Murdoch and Weiss⁷ with only small modification. One gram of $\text{Fe}_2(\text{CO})_9$ was placed in a 40 mL stainless steel bomb reactor with 10 mL of pentane. The bomb was charged with 30 atm of ethylene by condensing 1.2 L of ethylene at 1 atm into the bomb at -196°C . The reaction was run for at least 2 days and then the excess ethylene was vented and the solvent was removed under vacuum at -80°C . The rest of the sample manipulation was performed in a darkened laboratory, due to the high light sensitivity of this compound.¹⁷ Exposure to fluorescent light caused rapid decomposition as indicated by the production of a dark green compound ($\text{Fe}_3(\text{CO})_{12}$).

It is well-documented that one byproduct of this reaction, $\text{Fe}(\text{CO})_5$, is extremely difficult to remove^{10,13} from the product $\text{C}_2\text{H}_4\text{Fe}(\text{CO})_4$. Due to the nature of the microwave experiment, a highly pure sample was not necessary for measurements of strong microwave transitions. Therefore, a typical sample preparation involved only a partial separation of the products. After solvent removal under vacuum at -80°C , the bomb reactor was slowly warmed and the contents were removed under vacuum into two fractions. The first fraction, containing mostly pentacarbonyliron, was collected up to a temperature of -35°C . The second fraction, containing mostly tetracarbonylethyleneiron, was then collected from -35 to 0°C . At this point little or no material was observed to be leaving the bomb. Infrared analyses of the different fractions revealed significant amounts of each product in both fractions, and the overlap of peaks in the C–O and Fe–C stretching regions was significant.

Microwave measurements were made in the 4–12 GHz range using a Flygare-Balle type pulsed-beam Fourier transform microwave spectrometer.²⁸ The sample from the second fraction was maintained at -35°C , as the tetracarbonylethyleneiron was distilled into a small glass sample cell by applying vacuum through the attached pulsed valve and placing a small cup of liquid nitrogen (-196°C) around the sample cell. The pulse valve was then closed and the sample chamber filled with 1 atm of Ne carrier gas. The cell was warmed to 0°C . At lower frequencies a pressure of 1.5 atm was seen to increase signal intensity. Transitions measured are somewhat broadened due to unresolved Doppler components and perhaps even unresolved spin-rotation coupling. Greater broadening was observed for the perdeuterated sample, presumably due to unresolved quadrupole splitting. The standard deviations listed for the measured transitions listed in Tables 1–3 are 1 σ . Systematic errors in the frequencies are expected to be much less (1 part in 10^9) than the reported random errors because the spectrometer is periodically calibrated to the frequency standard broadcast from WWVH in Boulder, CO.

Interference was not expected from the major contaminant, iron pentacarbonyl, since it is not expected to exhibit a microwave spectrum because it has no permanent dipole moment. The microwave spectrum of $\text{C}_2\text{H}_4\text{Fe}(\text{CO})_4$ was most readily measured from the second fraction when the sample cell was held at 0°C . Evidence for $\text{Fe}(\text{CO})_5$ contamination in the early part of the experiment was revealed by a slowly growing signal intensity as the $\text{Fe}(\text{CO})_5$ distilled off. Often, after several hours of scanning the signal intensity would grow to 3–10 times the initial intensity, this would last for about an hour, and then the signal would drop to below half of the initial intensity. This behavior is attributed to the gradual fractionation of the more volatile $\text{Fe}(\text{CO})_5$ out of the sample chamber, leaving mostly $\text{C}_2\text{H}_4\text{Fe}(\text{CO})_4$. Since this molecule is highly volatile even at 0°C , the purified sample rapidly evaporates leaving only a small portion mixed with decomposition products. The primary decomposition products, ethylene and $\text{Fe}_3(\text{CO})_{12}$, are also volatile and can thus diminish signal intensity also. The samples were stored at -196°C , and appeared to be thermally stable up to -20°C for extended periods of time, but low volatility of $\text{C}_2\text{H}_4\text{Fe}(\text{CO})_4$ at this temperature required the scanning to be done above -10

- (15) Axe, F. U.; Marynick, D. S. *J. Am. Chem. Soc.* **1984**, *106*, 6230.
 (16) Li, J.; Schreckenbach, G.; Ziegler, T. *Inorg. Chem.* **1995**, *34*, 3245.
 (17) Albright, T. A.; Hoffman, R.; Thibeault, J. C.; Thorn, D. L. *J. Am. Chem. Soc.* **1979**, *101*, 3801.
 (18) Mitchener, J. C.; Wrighton, M. S. *J. Am. Chem. Soc.* **1983**, *105*, 1065.
 (19) Kukolich, S. G.; Sickafoose, S. M.; Breckenridge, S. M. *J. Am. Chem. Soc.* **1996**, *118*, 205.
 (20) Drouin, B. J.; Kukolich, S. G. *J. Am. Chem. Soc.* **1998**, *120*, 6774.
 (21) Lavaty, T. G.; Wikrent, P.; Drouin, B. J.; Kukolich, S. G. *J. Chem. Phys.* In press.
 (22) Roehrig, M. A.; Wikrent, P.; Huber, S. R.; Wigley, D. E.; Kukolich, S. G. *J. Mol. Spectrosc.* **1992**, *154*, 355.
 (23) Kukolich, S. G.; Breckenridge-Estes, S. M.; Sickafoose, S. M. *Inorg. Chem.* **1997**, *36*, 4916.
 (24) Drouin, B. J.; Cassak, P.; Kukolich, S. G. *Inorg. Chem.* **1996**, *36*, 2868.
 (25) Drouin, B. J.; Lavaty, T. G.; Cassak, P. A.; Kukolich, S. G. *J. Chem. Phys.* **1997**, *107*, 6541.
 (26) (a) Becke, A. D. *Phys. Rev.* **1988**, *A 38*, 3098. (b) *ACS Symp. Ser.* **1989**, *394*, 165. (c) *Int. J. Quantum Chem. Symp.* **1989**, *No. 23*, 599. (d) Perdew, J. P.; Wang, Y. *Phys. Rev.* **1992**, *B 45*, 13, 244.
 (27) Gaussian 94, Revision B.3; Frisch, M. J.; Trucks, G. W.; Schlegel, H. B.; Gill, P. M. W.; Johnson, B. G.; Robb, M. A.; Cheeseman, J. R.; Keith, T.; Petersson, G. A.; Montgomery, A. J.; Raghavachari, K.; Al-Laham, M. A.; Zakrzewski, V. G.; Ortiz, J. V.; Foresman, J. B.; Peng, C. Y.; Ayala, P. Y.; Chen, W.; Wong, M. W.; Andres, J. L.; Replogle, E. S.; Gomperts, R.; Martin, R. L.; Fox, D. J.; Binkley, J. S.; Defrees, D. J.; Baker, J.; Stewart, J. P.; Head-Gordon, M.; Gonzalez, C.; and Pople, J. A. Gaussian, Inc.; Pittsburgh, PA, 1995.

- (28) Bumgarner, R. E.; Kukolich, S. G. *J. Chem. Phys.* **1987**, *86*, 1083.

Table 1. Measured Transition Frequencies for $C_2H_4Fe(CO)_4$ and $C_2D_4Fe(CO)_4^a$

quantum nos.	$C_2H_4Fe(CO)_4$		$C_2D_4Fe(CO)_4$			
	$J_{K_p K_o}$	$J'_{K_p' K_o'}$	measured	dev	measured	dev
1 ₁₀ 2 ₂₀			3911.7638(18)	0.0007		
2 ₀₂ 3 ₁₂			5358.7201(37)	-0.0030	5125.5720(12)	0.0009
2 ₁₁ 3 ₂₁			5566.1820(09)	0.0009	5341.3113(24)	0.0098
2 ₁₂ 3 ₂₂			5672.7252(13)	-0.0012	5411.5415(66)	0.0161
3 ₂₂ 4 ₁₄			5804.2278(26)	0.0049		
2 ₂₀ 3 ₃₀			5986.7355(15)	0.0017	5697.4804(19)	-0.0038
2 ₂₁ 3 ₃₁			5995.3931(15)	0.0014	5701.1674(13)	-0.0055
3 ₁₂ 4 ₀₄			6200.1532(38)	-0.0001		
3 ₂₁ 4 ₁₃			6261.0940(42)	-0.0022		
4 ₄₁ 5 ₃₃			7001.0737(76)	0.0049		
4 ₄₀ 5 ₃₂			7032.7745(32)	-0.0029		
3 ₀₃ 4 ₁₃			7143.1090(23)	-0.0009	6814.7490(59)	0.0077
3 ₁₂ 4 ₂₂			7239.1109(27)	0.0013	6955.1697(40)	-0.0087
4 ₃₂ 5 ₂₄			7305.2943(67)	-0.0047		
4 ₂₃ 5 ₁₅			7319.6564(29)	0.0001		
3 ₁₃ 4 ₂₃			7415.8640(13)	0.0001	7078.4238(23)	-0.0065
4 ₃₁ 5 ₂₃			7562.5340(56)	-0.0034		
3 ₂₁ 4 ₃₁			7641.5320(19)	0.0004	7313.7021(38)	-0.0038
4 ₁₃ 5 ₀₅			7652.6716(11)	-0.0053		
3 ₂₂ 4 ₃₂			7680.3698(15)	-0.0004	7331.0333(53)	0.0056
5 ₃₂ 6 ₀₆			7700.6236(49)	0.0015		
4 ₂₂ 5 ₁₄			7926.9064(43)	-0.0003		
3 ₃₀ 4 ₄₀			8052.9087(24)	0.0019	7654.2221(29)	-0.0051
3 ₃₁ 4 ₄₁			8054.0011(21)	0.0020	7654.5402(08)	-0.0055
5 ₅₀ 6 ₄₂			8295.6270(49)	0.0031		
3 ₀₃ 4 ₃₁			8523.5437(15)	-0.0016		
5 ₃₃ 6 ₂₅			8907.1688(14)	0.0014		
4 ₁₃ 5 ₂₃			8942.9717(24)	-0.0012	8583.0771(30)	-0.0082
4 ₀₄ 5 ₁₄			8965.8631(35)	0.0001		
4 ₁₄ 5 ₂₄			9181.4488(19)	0.0025		
4 ₂₂ 5 ₃₂			9282.0181(89)	-0.0015	8920.5697(28)	-0.0012
4 ₂₃ 5 ₃₃			9379.6367(13)	-0.0001	8967.5165(90)	-0.0023
4 ₃₁ 5 ₄₁			9720.3487(51)	0.0009	9276.8988(55)	0.0019
4 ₃₂ 5 ₄₂			9727.5750(31)	-0.0019	9279.0550(26)	0.0006
5 ₂₃ 6 ₁₅					9368.7648(46)	-0.0010
4 ₄₀ 5 ₅₀			10115.6700(29)	-0.0006	9609.3683(17)	0.0072
4 ₄₁ 5 ₅₁			10115.7876(28)	0.0047		
5 ₁₄ 6 ₂₄			10685.0477(33)	0.0026	10230.8835(35)	-0.0038
5 ₀₅ 6 ₁₅			10816.2091(19)	-0.0013	10263.6681(70)	-0.0001
5 ₂₃ 6 ₃₃			10919.7230(15)	-0.0007	10518.7883(35)	0.0087
5 ₁₅ 6 ₂₅			10967.1489(14)	0.0010		
5 ₂₄ 6 ₃₄			11097.2505(42)	0.0007	10613.0840(69)	0.0015
5 ₃₂ 6 ₄₂			11378.5117(54)	-0.0054		
5 ₃₃ 6 ₄₃			11405.0018(22)	0.0024	10904.5500(73)	0.0016
5 ₄₁ 6 ₅₁			11786.3176(34)	-0.0013	11233.0694(69)	-0.0060
5 ₄₂ 6 ₅₂			11787.2907(27)	-0.0023	11233.2777(51)	0.0038
5 ₅₀ 6 ₆₀			12177.9478(21)	0.0014	11564.3312(35)	-0.0010

^a All measured frequencies and deviations (dev = measured - calculated) from calculated values are given in MHz, listed uncertainties in the measured lines are 1σ .

$^{\circ}C$. No signal was observed below $-20^{\circ}C$, the strongest signals were observed at $0^{\circ}C$, but no measurements were attempted at higher temperatures due to thermal instability of the compound.

The perdeuterated sample was prepared with perdeuterated ethylene- d_4 , obtained from Cambridge Isotopes. One liter of C_2D_4 was combined with 200 mL of C_2H_4 prior to condensation into the reaction vessel. The intensity of the main isotope signal was a small fraction of the $C_2D_4Fe(CO)_4$ signal intensity. All sample manipulation for the deuterated sample was identical with that for the normal isotopic species.

For measurements of the ^{18}O lines, it was necessary to further purify the sample prior to transfer into the spectrometer sample cell. The second fraction described above was slowly fractionated in a $-30^{\circ}C$ cold trap, and the remaining material was then used in the experiment. This purified sample gave up to 200:1 signal-to-noise ratios for the main isotope transitions. However, the increased volatility also caused rapid loss of sample during the experiment.

NMR spectra were recorded on a Unity 300 MHz NMR spectrometer at $0^{\circ}C$. The sample was vacuum distilled into the NMR tube along

with $CDCl_3$ solvent. The tube was sealed and stored at $-78^{\circ}C$ prior to running the experiment. The proton decoupling was turned off so that the $^{13}C-^1H$ spin-spin coupling constant could be determined. The center of the $^{13}C_{et}$ triplet was found at 34.9 ppm, in good agreement with the proton decoupled value²⁹ of 35.3 ppm. The 1:2:1 triplet pattern had a spin-spin splitting of $^1J_{CH} = 161(1)$ Hz. The 1H NMR spectrum showed a singlet at 2.48 ppm with ^{13}C sidebands at 155(5) Hz separation. Peaks due to the reaction solvent pentane were also observed at the same signal-to-noise ratio as the product compound.

Calculations. The DFT calculations were performed on an SGI Origin 2000 computer using the algorithms of Gaussian94 revision E.2.²⁷ The density functional methods of Becke^{26a-c} and Perdew and Wang^{26d} (BPW91) were applied for a geometry optimization of the structure of tetracarbonyl ethyleneiron. All coordinates were varied in both internal coordinate space and Cartesian coordinate space, each leading to an identical minimum that has all real positive vibrational frequencies, subject to C_{2v} symmetry constraint. The ground-state structure is in excellent agreement with previously published¹⁵ DFT results using the ADF³⁰⁻³² package; unfortunately, this study did not report the complete hydrogen atom coordinates.

Data Analysis: Microwave Spectra. The measured rotational spectrum for $C_2H_4Fe(CO)_4$ was successfully analyzed as an asymmetric top with only a "c"-type dipole moment. The measured lines are listed in Table 1 along with the quantum number assignments. The deviations of the "best fit" calculated transition frequencies from measured values are also included to demonstrate the ability of the model to reproduce the spectrum within experimental error. The lack of measured transitions for "a"- and "b"-type dipole selection rules provides strong evidence for the C_{2v} symmetry in this complex. After the "c"-type transitions were fit, the hypothetical "a"- and "b"-type transitions could be calculated with greater accuracy. Many of these predicted transitions are very close to regions containing "c" type transitions which had been extensively scanned in search of ^{13}C and ^{18}O transitions. The existence of only three sets of ^{13}C lines and two sets of ^{18}O lines further verifies that the three pairs of carbon atoms and two pairs of oxygen atoms lie in symmetry-related positions within the molecule. We therefore believe that only "c"-dipole transitions are possible for the main isotopomer.

The ^{13}C and ^{18}O transitions were measured in natural abundance (2.2% and 0.4%, respectively) using the normal isotope sample, and these are given in Tables 2 and 3. The perdeuterated sample was greater than 80% D_4 , so a variety of transitions were readily measured, and the transition frequencies are shown in Table 1 alongside the corresponding main isotope transitions.

The structure of this complex is shown in Figure 1. The a inertial axis is nearly in line with the axial carbonyl groups with the remaining ligands located in the equatorial plane. The c inertial axis is coincident with the C_2 rotation axis of the molecule and lies in the equatorial plane. The carbon atoms of the ethylene ligand lie in the bc (equatorial) plane. From here on the carbon atoms in the ethylene ligand will be referred to as C_{et} , and the carbon and oxygen atoms in the CO ligands will be referred to as C_{eq} , O_{eq} , C_{ax} , and O_{ax} , denoting the equatorial and axial carbonyls, respectively. Note that in Figure 1 the principal axes (abc) correspond directly to the symmetry axes (xyz) for the C_{2v} point group.

Measured rotational transitions were used in a nonlinear least-squares fitting routine to determine the adjustable parameters of an asymmetric top Hamiltonian with centrifugal distortion constants. The molecule exhibits a typical nearly rigid-rotor spectrum with all distortion constants well below 1 kHz. For the main isotopomer, many $\Delta K_0 = 2$ lines were measured along with one $\Delta K_0 = 4$ line and one $\Delta K_0 = -2$ line. These transitions helped to independently define the five quartic distortion

(29) Lindner, E.; Jansen, R. M.; Schauss, E. *Organometallic Syntheses*; Elsevier Publishing Co., Inc.: New York, 1988; Vol. 4, p 141.

(30) Baerends, E. J.; Ellis, D. E.; Ros, P. *Chem. Phys.* **1973**, 2, 41.

(31) Ravenek, W. *Algorithms and Applications on Vector and Parallel Computers*; Rilel, H. J. J., Dekkar, Th. J., van de Vorst, H. A., Eds.; Elsevier: Amsterdam, 1987.

(32) (a) Boerrigter, P. M.; te Velde, G.; Baerends, E. J. *Int. J. Quantum Chem.* **1988**, 33, 87. (b) te Velde, G.; Baerends, E. J. *J. Comput. Phys.* **1992**, 99, 84.

Table 2. Measured Transition Frequencies for the ^{13}C Substituted Isotomers Measured in Natural Abundance^a

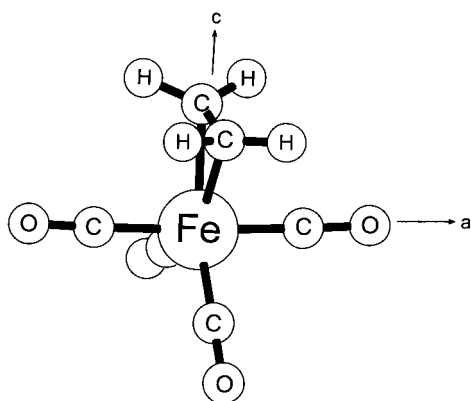
quantum nos. $J_{KpKo} J'_{Kp'Ko'}$	$^{13}\text{C}_{\text{et}}$		$^{13}\text{C}_{\text{eq}}$		$^{13}\text{C}_{\text{ax}}$	
	measured	dev	measured	dev	measured	dev
2 ₀₂ 3 ₁₂	5315.2613(34)	-0.0020	5347.3062(59)	0.0036	5334.3700(14)	-0.0004
2 ₁₁ 3 ₂₁	5526.5370(15)	-0.0024	5542.0028(41)	0.0029	5551.5284(15)	-0.0040
2 ₁₂ 3 ₂₂	5624.7603(56)	-0.0022	5649.6556(59)	-0.0015	5658.2690(09)	-0.0024
2 ₂₀ 3 ₃₀	5934.2677(25)	0.0014	5952.0154(07)	-0.0008	5982.1754(22)	-0.0015
2 ₂₁ 3 ₃₁	5941.5321(34)	-0.0008	5961.3871(24)	-0.0013	5990.5016(53)	0.0017
3 ₀₃ 4 ₁₃	7080.3191(64)	0.0008	7131.7376(54)	0.0014	7108.2804(53)	-0.0007
3 ₁₂ 4 ₂₂	7188.3418(71)	0.0035	7214.1885(13)	-0.0017	7213.5489(61)	0.0007
3 ₁₃ 4 ₂₃	7353.4343(41)	-0.0014	7391.0288(56)	0.0018	7391.6478(24)	-0.0077
3 ₂₁ 4 ₃₁	7584.0571(24)	-0.0014	7601.9490(53)	-0.0037	7628.3061(25)	0.0004
3 ₂₂ 4 ₃₂	7617.0483(06)	-0.0004	7643.5900(83)	-0.0005	7665.8476(44)	0.0024
3 ₃₀ 4 ₄₀	7980.0365(23)	-0.0020	8005.4959(59)	-0.0023	8048.1561(22)	0.0014
3 ₃₁ 4 ₄₁	7980.8854(15)	0.0009	8006.7527(61)	0.0006	8049.1690(15)	0.0006
4 ₁₃ 5 ₂₃	8876.8034(32)	0.0000	8919.1061(35)	-0.0049	8905.6748(30)	0.0014
4 ₀₄ 5 ₁₄	8880.5862(18)	0.0004	8954.8870(36)	-0.0005	8920.5855(65)	0.0011
4 ₁₄ 5 ₂₄	9102.5319(36)	-0.0007	9155.2956(14)	0.0007	9147.4008(19)	0.0041
4 ₂₂ 5 ₃₂	9220.2730(15)	0.0004	9237.9591(83)	0.0051	9259.8779(13)	0.0020
4 ₂₃ 5 ₃₃	9304.8082(32)	0.0028	9341.0192(31)	0.0015	9355.0506(73)	-0.0017
4 ₃₁ 5 ₄₁	9640.9731(20)	-0.0025	9668.5725(29)	-0.0013	9706.7121(52)	-0.0016
4 ₃₂ 5 ₄₂	9646.6097(37)	0.0006	9676.8247(32)	-0.0040	9713.4431(65)	0.0020
4 ₄₀ 5 ₅₀	10022.8825(82)	0.0079	10055.3688(84)	0.0044	10110.8257(37)	0.0089
4 ₄₁ 5 ₅₁	10022.9498(30)	-0.0053	10055.5018(65)	0.0008	10110.9077(46)	-0.0099

^a All measured frequencies and deviations (dev = measured - calculated) from calculated values are given in MHz, listed uncertainties are 1σ .

Table 3. Measured Transition Frequencies and Deviations from Calculated Values for ^{18}O Substituted Isotomers Measured in Natural Abundance^a

quantum nos. $J_{KpKo} J'_{Kp'Ko'}$	$^{18}\text{O}_{\text{eq}}$		$^{18}\text{O}_{\text{ax}}$	
	measured	dev	measured	dev
2 ₁₁ 3 ₂₁	5442.7813(62)	0.0071	5491.3845(67)	0.0043
2 ₂₀ 3 ₃₀	5803.4305(32)	-0.0045	5963.2893(02)	-0.0039
2 ₂₁ 3 ₃₁	5817.1347(66)	0.0003	5970.3676(62)	0.0023
3 ₀₃ 4 ₁₃	7094.2726(28)	-0.0019	7108.7282(37)	-0.0010
3 ₁₂ 4 ₂₂	7117.0123(32)	0.0017		
3 ₂₁ 4 ₃₁	7432.5862(24)	0.0100	7573.3379(64)	-0.0022
3 ₂₂ 4 ₃₂	7489.8100(52)	-0.0066	7605.8571(50)	-0.0001
3 ₃₀ 4 ₄₀	7803.0955(38)	0.0013	8028.5520(26)	0.0000
3 ₃₁ 4 ₄₁	7805.5376(29)	-0.0021	8029.3019(21)	0.0015
4 ₁₃ 5 ₂₃	8832.8068(34)	-0.0128		
4 ₀₄ 5 ₁₄	8920.1084(74)	0.0092		

^a All measured frequencies and deviations (dev = measured - calculated) from calculated values are given in MHz, listed uncertainties are 1σ .

**Figure 1.** The molecular structure and principal axis system for tetracarbonyl ethyleneiron. The axial carbonyl groups are at an angle of 2.6° relative to the "a" principal axis.

constants. The parameter δ_j could only be determined using all the available data, and the small value of 6(5) Hz indicates that it makes a negligibly small contribution to "regular" $\Delta K_o = 0$ transitions. The value of δ_j was fixed at zero during all of the isotopically substituted spectral fits. For the ^{18}O isotopomers, only a limited data set was

available, thus all of the distortion constants were held fixed at the values obtained for the main isotopomer, since these values are not expected to change much upon isotopic substitution. For the ^{13}C isotopomers the parameters D_j and D_{JK} could each be treated as variable parameters to obtain values in agreement with the main isotopomer values. To reduce correlation errors in the rotational constants for these species all of the distortion constants were fixed at main isotopomer values for the final fits. For the perdeuterated species only D_{JK} was fixed at the value for the main isotopomer. The value for D_{JK} was not well determined in the fit, presumably due to the lack of $\Delta K_o = 2$ transitions and the larger uncertainties in the line centers caused by unresolved deuterium quadrupole coupling. The Hamiltonian parameters obtained from the least-squares fitting analyses and the standard deviations of the fits are given in Table 4.

Molecular Structure. Data were collected on 7 isotopomers and therefore 21 rotational constants were used for the structural analyses. Two structures can be determined from the spectral data: Kraitchman (r_s) and least squares (r_o). The Kraitchman structure, which gives only coordinates of isotopically substituted atoms, is incomplete without ^{54}Fe substitution data. However, the iron c coordinate for the r_s structure can be obtained through the first moment equation for the c axis. The least-squares structure also allows complete determination of all atomic coordinates. The r_o , or least-squares, structure was determined by two independent methods denoted methods "a" and method "b". In method a, the *internal* coordinates of the molecule, defined by bond lengths, interbond angles, and Cartesian coordinates, are varied as parameters in a least-squares fit to the *rotational constants*. Method b employs the program written by Schwendeman,³³ in which the *Cartesian* coordinates are varied in a fit to the experimental *moments of inertia*. Both r_o structures are in excellent agreement with each other, with the Kraitchman structure, and with the theoretical structure obtained using DFT.

Kraitchman Analysis. The substitution coordinates directly determined from Kraitchman's equations are given in Table 5. For the quadruple substitution of the four equivalent hydrogen atoms it was necessary to develop substitution coordinate equations from first principles. In general, the differences between the inertial moments for the main and (multiply) substituted species can be expressed³⁴ as

(33) Schwendeman, R. H. *Critical Evaluation of Chemical and Physical Structural Information*; Lide, D. R.; Paul, M. A., Eds.; National Academy of Sciences: Washington, DC, 1974; p 74. Thanks to Kurt Hillig for continued updates of the code.

(34) Gordy, W.; Cook, R. L. *Microwave Molecular Spectra*; Interscience Publishers: John Wiley & Sons: New York, 1970; Chapter 13.

Table 4. Rotational Constants Derived from the Measured Transition Frequencies^a

parameter	C ₂ H ₄ Fe(CO) ₄	¹³ C _{et}	¹³ C _{ax}	¹³ C _{eq}	¹⁸ O _{ax}	¹⁸ O _{eq}	D ₄
A, MHz	1031.1079(4)	1021.2044(4)	1031.0759(5)	1024.6218(4)	1030.9689(5)	996.9317(15)	977.4884(15)
B, MHz	859.8056(4)	853.7213(4)	855.0194(5)	858.6021(4)	835.1063(6)	854.5308(14)	826.3590(16)
C, MHz	808.5672(4)	807.8437(11)	804.3557(17)	805.6373(12)	786.7757(19)	791.8870(60)	796.3847(22)
D _J , KHz	0.094(7)	0.094(F)*	0.094(F)*	0.094(F)*	0.094(F)*	0.094(F)*	0.12(2)
D _{JK} , KHz	0.10(3)	0.10(F)*	0.10(F)*	0.10(F)*	0.10(F)*	0.10(F)*	0.10(F)*
D _K , KHz	-0.17(2)	-0.17(F)*	-0.17(F)*	-0.17(F)*	-0.17(F)*	-0.17(F)*	-0.17(4)
δ _J , Hz	6(5)	6(F)*	6(F)*	6(F)*	6(F)*	6(F)*	6(F)*
δ _K , KHz	0.37(5)	0.37(F)*	0.37(F)*	0.37(F)*	0.37(F)*	0.37(F)*	0.4(2)
σ _{fit} , KHz	2.6	2.8	4.1	2.8	2.8	7.7	6.7

^a The Hamiltonian models an asymmetric top with five independent distortion constants. All errors in parameters are 2σ. The value of δ_J was held fixed at zero for all substituted isotopomer fits. Asterisks with (F) indicate fixed at values obtained in fitting the normal isotopomer.

Table 5. Results of the Cartesian Coordinate Least-Squares Structure Fit to the Experimental Moments of Inertia (Standard deviation of fit 0.004 amu·Å², or 28 kHz) and the Kraitchman Analysis Showing Absolute Values of Substituted Atom Coordinates in the Parent (FeH₂(CO)₄) Principal Axis System (see Figure 1). (Uncertainties near 0.003 Å)^a

atom	a _o (Å)	b _o (Å)	c _o (Å)	a _s (Å)	b _s (Å)	c _s (Å)	r _{com} (Å)
Fe	0.000 ^a	0.000 ^b	0.073(16)			0.081	
C _{ax}	±1.814(2)	0.000 ^b	0.148(32)	1.8107	0.043i ^c	0.132	1.816
O _{ax}	±2.954(1)	0.000 ^b	0.205(14)	2.9535	0.048i ^c	0.199	2.960
C _{eq}	0.000 ^b	±1.496(3)	-0.942(4)	0.052i ^c	1.493	0.937	1.762
O _{eq}	0.000 ^b	±2.448(1)	-1.576(2)	0.043i ^c	2.448	1.574	2.902
C _{et}	0.000 ^b	±0.709(3)	2.067(2)	0.059i ^c	0.706	2.064	2.182
H	±0.897(2)	±1.254(1)	2.2835(6)	0.896	1.254	2.283	2.755

^a Listed errors are 2σ. ^b These values were fixed at zero during the fitting. ^c These coordinates are nonzero (and/or imaginary) due to vibrational averaging.

shown in eq 1:

$$\Delta I_{aa} = \Delta m(b_s^2 + c_s^2) - \frac{(\sum_i \Delta mb_i)^2}{M + \Delta m} - \frac{(\sum_i \Delta mc_i)^2}{M + \Delta m} \quad (1)$$

where Δ*m* is the difference between the total mass of the parent (*M*) and the substituted isotopomer. The subscript *s* refers to the coordinates of the substituted atom(s). The second and third terms account for the shift of the center of mass from the parent molecule. The analogous terms for Δ*I*_{bb} and Δ*I*_{cc} can be obtained by cyclic permutation of the *abc* coordinates in eq 1. For single substitution, the second and third terms are typically combined with their corresponding substitution coordinate to give a single term involving the substitution reduced mass, μ = Δ*m*·*M*/(Δ*m* + *M*). In some cases, where multiple substitution retains the initial symmetry of the parent molecule it is possible that these terms will drop out of the difference moment equations entirely. The C_{2v} symmetry of tetracarbonyl ethyleneiron gives the molecule both *ac* and *bc* mirror planes. The *ac* mirror plane forces the second term in Δ*I*_{aa} to zero, thus the first term is all that contributes to the *b*_H coordinate. Similarly, symmetry about the *bc* plane cancels the corresponding term in Δ*I*_{bb}, and together these mirror planes cancel both terms in Δ*I*_{cc}. The third term in Δ*I*_{aa} and Δ*I*_{bb} remains, and when combined with Δ*m*c_s² can be shown to reduce to μ. Therefore, the difference moments for quadruple deuterium substitution in this molecule can be expressed as:

$$\Delta I_{aa} = \Delta mb_H^2 + \mu c_H^2, \Delta I_{bb} = \Delta ma_H^2 + \mu c_H^2, \Delta I_{cc} = \Delta m(a_H^2 + b_H^2); \Delta m = 4(m_D - m_H) \quad (2)$$

Since the quadruple substitution does not rotate the principal axes there are no off-diagonal terms in the inertial tensor for the substituted molecule. This allows for rapid solution of the three difference moments in eq 1 to give the hydrogen substitution coordinates:

$$|a| = \sqrt{\frac{\Delta I_{bb} + \Delta I_{cc} - \Delta I_{aa}}{2\Delta m}}, |b| = \sqrt{\frac{\Delta I_{cc} + \Delta I_{aa} - \Delta I_{bb}}{2\Delta m}}, |c| = \sqrt{\frac{\Delta I_{aa} + \Delta I_{bb} - \Delta I_{cc}}{2\mu}} \quad (3)$$

The carbon and oxygen atom positions obtained using the Kraitchman equations for single substitution in an asymmetric top, the program of Schwendeman,³³ and one developed in this laboratory produced identical results. It should be noted that the Kraitchman coordinates for atoms in the *ac* and *bc* planes that should be zero are in fact nonzero or imaginary. This effect is similar to inertial defects in planar molecules in which zero-point vibrational movement of the atoms out of the plane results in substitution coordinates that represent the root-mean-square average vibrational displacements. In this molecule, the Kraitchman analysis provides root-mean-square positions for the *b* coordinates of atoms in the *ac* plane and the *a* coordinates of atoms in the *bc* plane. The iron atom is the only nonsubstituted atom in the molecule; therefore all of the substituted atom *c*_s coordinates can be used to solve the *c* axis first moment equation for the iron *c* coordinate. For the internal coordinates listed in Table 6, it was necessary to assume all of the small nonzero "out of plane" values to be zero. The errors reported for internal substitution coordinates are derived from Costain's³⁵ model by using the Schwendeman program.

Least-Squares Analyses. Two independent least-squares fitting methods were employed in an effort to minimize errors resulting from correlation between variable parameters and from inherent weighting of experimental data.

In method a the internal coordinates of the molecule were defined using the Fe-C_{ax}, Fe-C_{eq}, C_{ax}-O_{ax}, C_{eq}-O_{eq}, Fe-C_{et}, and C_{et}-C_{et} bond lengths and the ∠C_{ax}-Fe-C_{ax}, ∠C_{eq}-Fe-C_{eq}, ∠Fe-C_{ax}-O_{ax}, ∠Fe-C_{eq}-O_{eq} interbond angles; the hydrogen Cartesian coordinates were varied as three independent parameters. Within the C_{2v} symmetry of the molecule this scheme allowed variation of 13 independent molecular parameters in a fit to the 21 measured rotational constants. The standard deviation of the fit was 11 kHz, indicating that the final structure reproduces the experimental rotational constants to within 1 order of magnitude of their experimental error (~1 kHz). Final values of the variable parameters and other interesting structural parameters are given in Table 6.

In method b, the Cartesian coordinates of symmetrically related atoms were tied together to give 13 independent parameters; the location of the iron atom along the *c* inertial axis was a 14th dependent parameter in the fit. Each set of carbon atoms required two variables (*b* and *c* for C_{et} and C_{eq}, *a* and *c* for C_{ax}), similarly the two sets of oxygen atoms each required two variables, finally the H atoms required 3 variables

Table 6. Structural Parameters Derived from the Experimental Rotational Constants^a(a) Bond Lengths Determined in Structural Fits (a) and (b) and with Kraitchman's Equations and $c(\text{H}-\text{C})$, the Separation between the Plane of the Ethylene H Atoms and the C-C Bond

bond	r_a (Å)	r_b (Å)	r_s (Å)
$r(\text{C}-\text{H})$	1.071(4)	1.072(3)	1.073(2)
$r(\text{Fe}-\text{C}_{\text{ax}})$	1.815(2)	1.815(2)	1.811(1)
$r(\text{Fe}-\text{C}_{\text{eq}})$	1.805(9)	1.807(9)	1.808(10)
$r(\text{Fe}-\text{C}_{\text{et}})$	2.118(14)	2.116(14)	2.105(17)
$r(\text{C}_{\text{et}}-\text{C}_{\text{et}})$	1.420(6)	1.418(8)	1.412(3)
$r(\text{C}_{\text{ax}}-\text{O}_{\text{ax}})$	1.142(2)	1.142(3)	1.145(2)
$r(\text{C}_{\text{eq}}-\text{O}_{\text{eq}})$	1.145(2)	1.145(4)	1.147(2)
$r(\text{Fe}-\text{H})$	1.996(14)	1.994(17)	1.983(17)
$c(\text{H}-\text{C})$	0.217(2)	0.217(2)	0.219(3)

(b) Interbond and Dihedral Angles Determined in Structural Fits (a) and (b) and with Kraitchman's Equations

angle	Θ_a (°)	Θ_b (°)	Θ_s (°)
$\angle\text{C}-\text{C}-\text{H}$	120.5(6)	120.6(3)	120.7(1)
$\angle\text{H}-\text{C}-\text{H}$	113.7(6)	113.6(5)	113.3(2)
$\angle\text{Fe}-\text{C}-\text{C}-\text{H}$	103.6(9)	103.6(9)	103.7(10)
$\angle\text{C}_{\text{ax}}-\text{Fe}-\text{C}_{\text{ax}}$	174.8(25)	175.3(19)	176.8(13)
$\angle\text{C}_{\text{eq}}-\text{Fe}-\text{C}_{\text{eq}}$	111.8(9)	111.6(8)	111.4(9)
$\angle\text{C}_{\text{et}}-\text{Fe}-\text{C}_{\text{et}}$	39.2(5)	39.2(4)	39.2(3)
$\angle\text{Fe}-\text{C}_{\text{ax}}-\text{O}_{\text{ax}}$	180.0(28)	179.5(30)	178.2(12)
$\angle\text{Fe}-\text{C}_{\text{eq}}-\text{O}_{\text{eq}}$	179.5(7)	179.4(6)	179.4(5)

^a Values determined in the internal/Cartesian coordinate least-squares fit to the rotational constants are denoted by a subscript "a". Values determined by a global Cartesian fit to the first and second moments of inertia are denoted by a subscript "b". Values obtained from Kraitchman's equations are denoted by the subscript "s". Errors for the least-squares fits "a" and "b" are 2σ , errors in Kraitchman coordinates are Costain³⁵ errors.

(a , b , and c coordinates). The 14 Cartesian coordinate parameters were varied to fit the 21 measured moments of inertia and forced to satisfy the first moment equation for c coordinates. The fit has a standard deviation of $0.0036 \text{ amu}\cdot\text{Å}^2$, which gives a relative uncertainty on the same order of magnitude (1×10^{-5}) as the standard deviation obtained in method a. The coordinates from method b and their respective uncertainties are listed in Table 5 alongside the Kraitchman values.

The experimental microwave bond lengths and angles determined from the two methods are given in Table 6. All three methods are in excellent agreement with each other, indicating that differences in correlation and weighting do not cause significant problems in the structural fits. The close agreement of the Kraitchman parameters with the least-squares structures indicates that the equilibrium values of the structural parameters are not very different from the reported r_o and r_s values. Unlike the similar compound $\text{H}_2\text{Fe}(\text{CO})_4$, the assumption of rigid bonding upon isotopic substitution seems to be accurate even in the hydrogenic coordinates of the ethylene ligand.

Discussion

This paper presents the first detailed study of the structural changes of ethylene upon complexation to iron. The displacement of the plane of the ethylene hydrogen atoms away from the ethylene C-C bond provides details of changes in bonding and hybridization of the ethylene moiety. This displacement was assumed to be small, but not accurately determined in previous studies. The interbond angles for the $\text{Fe}(\text{CO})_4$ fragment of this complex are considerably different than the corresponding angles for $\text{H}_2\text{Fe}(\text{CO})_4$. Bond lengths were found in excellent agreement with GED data whereas bond angles were determined with better accuracy and precision in the present work. Theoretical treatment using DFT provided a very reliable structure for the search and subsequent analysis of the microwave spectra.

The DFT study presented here is a remarkable example of theory supporting experiment. During the initial phase of scanning for microwave spectra, two predictions were obtained: one given by the published GED structure and one from the present DFT(BPW91) calculation. The two structures had very similar $(A + B)/2$ values, but very different $(B - C)/2$ values. This encouraged us to look for the $\Delta J = +1$ $K_o = 0, 1$ transitions that were predicted to be very close to each other. The distance between the two K_o transitions could give a better value for $(B - C)/2$ and the overall location and spacing between consecutive ΔJ transitions (R branches) could give a better value for $(A + B)/2$. The $J' \leftarrow J = 3 \leftarrow 2$, $K_o = 0, 1$ transitions were predicted 30 MHz apart for the two structures, and were found between the two predictions, closer to the DFT prediction. The measured splitting between the two K_o components (9 MHz) is also much closer to the DFT prediction (5 MHz) than the GED prediction (1 MHz). After accurate determination of the main isotopomer parameters, an approximate structure fit was done, allowing only the $\text{Fe}-\text{C}_{\text{et}}$ and $\text{C}_{\text{et}}-\text{C}_{\text{et}}$ distances to vary, and holding all other parameters fixed at values from the DFT structure. This resulted in a surprisingly accurate structure that allowed prediction of the ^{13}C lines to within 2 MHz for most transitions of all the ^{13}C -substituted isotopomers. The new data set containing ^{13}C coordinates was quite insensitive to the location of the hydrogen atoms, and thus a reliable prediction for the quadruply substituted D_4 complex was a concern. A study of the dependence of the least-squares fit standard deviations on the C-C-H and Fe-C-C-H angles showed a flat surface with a shallow minimum very close to the DFT prediction. The structure corresponding to this minimum was used to predict the D_4 substituted spectrum. This proved to be an accurate analysis since the D_4 -substituted transitions were found within 3 MHz of the predicted frequencies. This indicates that the DFT structure obtained using the functionals described by Becke, Perdew, and Wang²⁶ is a very accurate representation of the gas-phase structure of this compound. In comparison to the ADF DFT^{31,32} (using the B3LYP functional) work,¹⁶ the reported parameters are in good agreement for the C_{ax} and C_{et} bond lengths and angles. The calculated $\text{Fe}-\text{C}_{\text{eq}}$ and $\text{Fe}-\text{C}_{\text{ax}}$ bond lengths are nearly equal (agree within experimental error). This result is in better agreement with the experiment than the present DFT study. The only reported parameter for hydrogen atoms is the dihedral angle describing the bending of the C-H bond out of the former ethylene plane. The B3LYP method gives an Fe-C-C-H dihedral angle of 111.5° which is significantly larger than the experimental value. This would indicate that the BPW91 methods may better represent small structural changes upon olefin complexation. It is also interesting to note that the least well-determined parameter in the DFT study is the $\text{Fe}-\text{C}_{\text{et}}$ distance, which also has the largest uncertainty in the experimental work. This is an indication of the diffuse metal-olefin bonding. The electronic structure calculations give the most difficulty with the metal-olefin bonding, and the rotation of the molecule evidently causes more centrifugal distortion along this coordinate. Despite these difficulties, the $\text{Fe}-\text{C}_{\text{et}}$ bond length was determined to 1% accuracy.

There are some discrepancies in the literature^{11,13,15-17} concerning the iron-carbon bond lengths for the carbonyl ligands in tetracarbonyl ethyleneiron. It is well-known that the "piano-stool" compounds with η^4 bound olefins have remarkably different Fe-C bond lengths and Fe-C-O interbond angles in the iron tricarbonyl base. In $\text{H}_2\text{Fe}(\text{CO})_4$ either intermolecular exchange or intramolecular pseudorotation causes

Table 7. Structural Parameters Obtained in This and Various Other Studies of Tetracarbonylethyleneiron and of the Closely Related Species Triphenylphosphinetricarbonylethyleneiron

structural parameter	C ₂ H ₄ Fe(CO) ₄ GED	C ₂ H ₄ XFe(CO) ₄ X-ray ^b	C ₂ H ₄ Fe(CO) ₄ MW ^c	C ₂ H ₄ Fe(CO) ₄ DFT
$r(\text{Fe}-\text{C}_{\text{et}})$ (Å)	2.117(30)	2.099(7) ^b	2.117(14)	2.1188
$r(\text{Fe}-\text{C}_{\text{ax}})$ (Å)	1.796(35)	1.759(6)	1.815(2)	1.8006
$r(\text{Fe}-\text{C}_{\text{eq}})$ (Å)	1.836(35)	1.761(6) ^b	1.806(9)	1.7865
$r(\text{C}_{\text{et}}-\text{C}_{\text{et}})$ (Å)	1.46(6)	1.398(8)	1.419(7)	1.4186
$r(\text{C}_{\text{ax}}-\text{O}_{\text{ax}})$ (Å)	1.146(10)	1.164(4)	1.142(3)	1.1546
$r(\text{C}_{\text{eq}}-\text{O}_{\text{eq}})$ (Å)	1.146(10)	1.171(12) ^b	1.145(3)	1.1576
$r(\text{C}-\text{H})$ (Å)	1.08 ^a	1.00(24) ^b	1.072(4)	1.0905
$\angle(\text{C}_{\text{et}}-\text{Fe}-\text{C}_{\text{et}})$ (°)	40.3	38.9(2)	39.2(5)	39.12
$\angle(\text{X}-\text{Fe}-\text{C}_{\text{ax}})$ (°)	180 ^a	176.4(2)	175.1(22)	176.64
$\angle(\text{C}_{\text{eq}}-\text{Fe}-\text{C}_{\text{eq}})$ (°)	105.2(30)	112.2(3)	111.7(9)	111.66
$\angle(\text{Fe}-\text{C}_{\text{ax}}-\text{O}_{\text{ax}})$ (°)	180 ^a	178.8(6)	179.8(29)	179.64
$\angle(\text{Fe}-\text{C}_{\text{eq}}-\text{O}_{\text{eq}})$ (°)	180 ^a	175.2(9) ^b	179.5(7)	180.27
$\angle(\text{C}-\text{C}-\text{H})$ (°)	116 ^a	118(8)	120.6(5)	120.0
$\angle(\text{Fe}-\text{C}-\text{C}-\text{H})$ (°)	90 ^a	98	103.6(9)	103.5

^a These values were assumed during the fitting process. ^b X = P(C₆H₅)₃. The compound is not symmetric, thus averaged values of symmetry related terms are listed; the number in parentheses represents the range if larger than 4σ. ^c This column lists average values of methods “a” and “b” described in the text.

the CO groups to appear equivalent on the NMR³⁶ time scale. A ¹³C NMR study²⁹ of tetracarbonylethyleneiron also shows a single peak at 212 ppm for *both* sets of carbonyl groups, indicating either an accidental chemical shift equivalence or that an exchange process is occurring on the longer time scale of the NMR experiment. The present experimental data, which include two sets of ¹³C carbonyl isotopomers, indicates that this complex is fairly rigid (no tunneling splittings were directly observed) and has two distinctly different locations for the two carbonyl groups, as was observed for H₂Fe(CO)₄.¹⁹ Interestingly, the iron carbon bond lengths were found to be equal to within experimental error. In the GED work an attempt was made to separate these bond lengths, but the final values reported in that study still have overlapping error bars. Furthermore, the theoretical studies (including this one) have all indicated small differences between these bond lengths. It should be noted that the theoretical predictions for the differences in bond lengths are in the opposite direction to the GED assignment, but do agree with the trend indicated by the present data. The present experimental data suggest errors for these bond lengths to be 0.009 and 0.002 Å for $r(\text{Fe}-\text{C}_{\text{ax}})$ and $r(\text{Fe}-\text{C}_{\text{eq}})$, respectively, and suggest that the two bond lengths are equal to within 0.01 Å. The DFT value for the difference in bond lengths is (0.014 Å) right at the error limit of the experiment, and thus there is not yet a definitive answer as to whether these bond lengths are equivalent to less than one hundredth of an angstrom. The Fe–C–O angles were very nearly linear for both groups. Both carbonyl groups were found to have collinear CO and Fe–C bonds to within 1°. The Fe(CO)₄ fragment has a structure much closer to the Fe(CO)₅ molecule than to H₂Fe(CO)₄.¹⁹ The trigonal bipyramid structure of C₂H₄Fe(CO)₄ deviated from the *D*_{3h} structure of Fe(CO)₅ primarily in the contraction of the C_{eq}–Fe–C_{eq} interbond angle from 120° to 111.7(9)°. The C_{ax}–Fe–C_{ax} bond angle deviates from linearity by 5(2)°. The C_{2v} distortions are more pronounced in H₂Fe(CO)₄ where the C_{eq}–Fe–C_{eq} and C_{ax}–Fe–C_{ax} angles are 99(4)° and 154(4)°, respectively.¹⁹ The Fe–C_{ax,eq} bond lengths in all three iron carbonyl compounds are nearly identical at 1.81 Å.

The results of the experimental and theoretical analyses indicate that the effects of complexation on ethylene are primarily the movement of the plane of the ethylene hydrogen atoms away from the carbon–carbon bond and elongation of

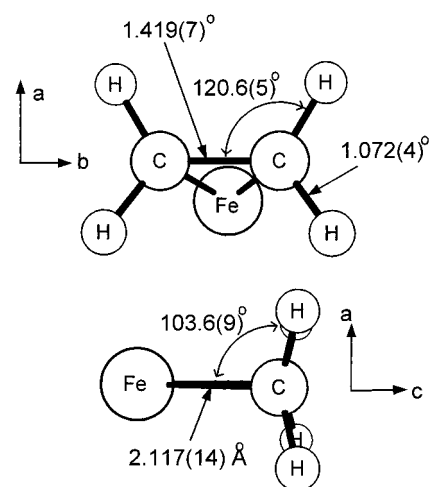


Figure 2. Structural parameters and internal coordinates for tetracarbonylethyleneiron showing the iron–ethylene fragment of the complex. In the top view, ethylene parameters are shown. In the bottom view, the iron–carbon bond length (2.117 Å) and the dihedral angle (103.6°), which would be 90° if the ethylene moiety remained planar, are shown.

the C–C bond length. There are only very minor changes in the C–H bond length and C–C–H bond angle (see Figure 2). The C–C bond is lengthened 0.07(1) to 1.419(7) Å, compared to 1.339(1) Å for free gaseous ethylene.³⁷ The previously reported GED value¹¹ (see Table 7) was much closer to a single C–C bond length, whereas this study produces a more accurate value, intermediate between typical single and double C–C bond lengths. The C–C–H angles of C₂H₄ and C₂H₄Fe(CO)₄ are nearly identical at 121.1(3)° and 120.6(5)°. The C–H bond lengths of 1.085(2) and 1.072(4) Å for C₂H₄ and C₂H₄Fe(CO)₄, respectively, demonstrate only a small contraction of 0.012(4) Å. To the authors’ knowledge, only one other experimental study¹³ of an ethylene–iron complex has determined the dihedral angle that describes the out-of-plane bend of the C–H bond. This X-ray diffraction study of triphenylphosphinetricarbonylethyleneiron determined this angle to be near 8°. The uncertainties in hydrogen coordinates in X-ray diffraction studies are often quite high, as can be seen by the erratic C–H bond lengths reported¹³ (see Table 7). An unperturbed ethylene structure would have the C–H bond “in the plane” perpendicular to the plane containing the Fe atom and the C_{et}–C_{et} bond. This

(36) Vancea, L.; Graham, W. A. G. *J. Organomet. Chem.* **1977**, *134*, 219.

(37) Duncan, J. L.; Wright, I. J.; Van Lerberghe, D. *J. Mol. Spectrosc.* **1972**, *42*, 463.

structure would have an Fe–C–C–H dihedral angle of 90°. The value determined in the present study, 103.6(9)°, is nearly halfway between what would be expected (120°) for full sp³ hybridization of the C_{et} atoms and unperturbed ethylene. An intermediate hybridization model is consistent with theory describing cyclopropane,³⁸ in the respect that the bonds characterized by small angles between ring atoms retain some π character. There is a crystal structure of the isoelectronic compound, tetracarbonyl-ethyleneosmium,³⁹ in which the ethylene appears to be more tightly bound to the metal center as indicated by an even larger C–C bond length of 1.488 Å (which would be much closer to sp³-type C–C bond lengths) and a larger “out-of-plane” bending of the hydrogens to ∠Os–C–C–H = 112°.

The values for the tetracarbonyl-ethyleneiron proton chemical shift (2.48 ppm) and ¹³C_{et} chemical shift (35 ppm) both fall between values for ethane (¹H 0.8 ppm, ¹³C 5.3 ppm) and ethylene (¹H 5.3 ppm, ¹³C 122 ppm). This is a further indication that the hybridization of ethylene, when complexed to iron, falls between sp³ and sp² hybridization.

Although arguments have been made⁴⁰ for correlations of the ¹³C–¹H spin–spin coupling constants (¹J_{CH}) with percent s character in the hybridized carbon orbitals at the carbon atom, the measured value of ¹J_{CH} = 161(1) Hz for the present iron complex indicates that the electronic structure (i.e., the percent s character) near the C_{et} atoms is very similar to that of free ethylene. Ethylene in CDCl₃ solvent⁴¹ has a coupling constant of ¹J_{CH} = 156.3 Hz. The values for ¹J_{CH} for sp³ hybridization are smaller (125 Hz). The coupling constant results do not give a good indication of the hybridization at carbon, which could be caused by interactions with the iron orbitals.

A qualitative inspection of valence orbitals indicates that the interaction of ethylene π and π* orbitals with d metal orbitals stabilizes the sp²-type configuration. An sp³ hybridization

scheme places the bonding orbitals outside the triangle formed by Fe and the two C_{et}'s; however, the sp² hybridization scheme places these partially within this triangle, thus allowing better overlap with the metal orbitals. An intermediate hybridization scheme allows favorable overlap between ligand and metal orbitals and gives the correct displacement of the H atoms. The H atom displacement may be an important part of the mechanism for catalytic isomerization of olefins. With the H atoms displaced out of the former ethylene plane, adjacent, bound olefin molecules can approach the ethylene more closely. With symmetry restrictions⁴² on olefin 2+2 addition removed, the olefin exchange process can proceed.

Summary

The complete, three-dimensional structure of tetracarbonyl-ethyleneiron was obtained by fitting and Kraitichman analysis of high-resolution microwave spectra for seven isotopomers. This is the first study of an organometallic complex for which a significant number of transitions have been obtained for natural-abundance ¹⁸O isotopomers. The structure of the ethylene is modified through interaction with the iron tetracarbonyl moiety. The C–C bond length for the complex is elongated by 0.07(1) Å relative to free ethylene and the plane of the ethylene H atoms is displaced 0.217(2) Å away from the C–C bond. The C–H bond length is reduced by 0.012(4) Å in the complex. These effects are in excellent agreement with the results of the DFT calculations. There are important correlations between structures and reactivity. The changes in the ethylene geometry observed here would correlate with reduced steric hindrance and increased reactivity with another complexed olefin. The present results should increase confidence in using DFT calculations for larger organometallic complexes.

Acknowledgment. We are extremely grateful to the National Science Foundation (Grant CHE-9634130) for support of this research. We thank Caroline Kriss for obtaining NMR spectra. Jennifer Dannemiller, Paul A. Cassak, and Burzin Engineer provided help with some of the spectra.

JA983937X

(42) Hoffman, R.; Woodward, R. B. *J. Am. Chem. Soc.* **1965**, *87*, 2046.

(38) Coulson, C. A.; Goodwin, T. H. *J. Chem. Soc.* **1971**, *93*, 1904.

(39) Bender, B. R.; Norton, J. R.; Miller, M. M.; Anderson, O. P.; Rappe, A. K. *Organometallics* **1992**, *11*, 3427.

(40) Muller, N.; Pritchard, D. E. *J. Chem. Phys.* **1959**, *31*, 1471.

(41) Lynden-Bell, R. M.; Sheppard, N. *Proc. R. Soc. London A* **1962**, *269*, 385.